

Electronic supplementary information

Hydrogenation of 2-methyl-3-butyn-2-ol over a Pd/ZnO catalyst: kinetic model and selectivity study

S. Vernuccio,^a R. Goy,^b Ph. Rudolf von Rohr,^a J. Medlock,^b and W. Bonrath^b

^aInstitute of Process Engineering, ETH Zurich, Sonneggstrasse 3, 8092 Zurich, Switzerland

^bDSM Nutritional Products, Research and Development, Basel, Switzerland

Physical properties

The physical properties of MBY, measured by DSM Nutritional Products at Kaiseraugst/Switzerland are listed in Tab. S1.

Table S1 Physical properties of MBY

T K	Density, ρ_L $\text{kg}\cdot\text{m}^{-3}$	Viscosity, $\mu_L\cdot 10^3$ Pa·s	Vapor pressure, p^0 bar
313	843	1.79	0.05
333	821	1.04	0.16
343	809	0.82	0.25
353	798	0.66	0.39

Catalyst characterization

Sections of EDX spectra of the SEM image reported in Fig. 1 (b) of the manuscript are showed in Fig. S1. EDX data were collected within the inspection fields marked in red.

Image (b1) reveals that the metal support comprises mainly iron, nickel and molybdenum according to the material composition of the EOS MaragingSteel MS1.

Although the EDX profile usually contains some background signal from surrounding areas, zinc and aluminium are only present in the coating layer (b2) and on the surface of the particle (b3).

Palladium signals appear only on the white spots decorating the external surface of the particle.

In Fig. S2 sections of EDX spectra recorded in the red inspection fields of STEM image in Fig. 2 (a) are shown as well. The inspection fields placed on presumed Pd nanoparticles clearly show the peak corresponding to Pd at about 3 kV. A pure Pd signal was never obtained due to the underlying or adjacent metallic support.

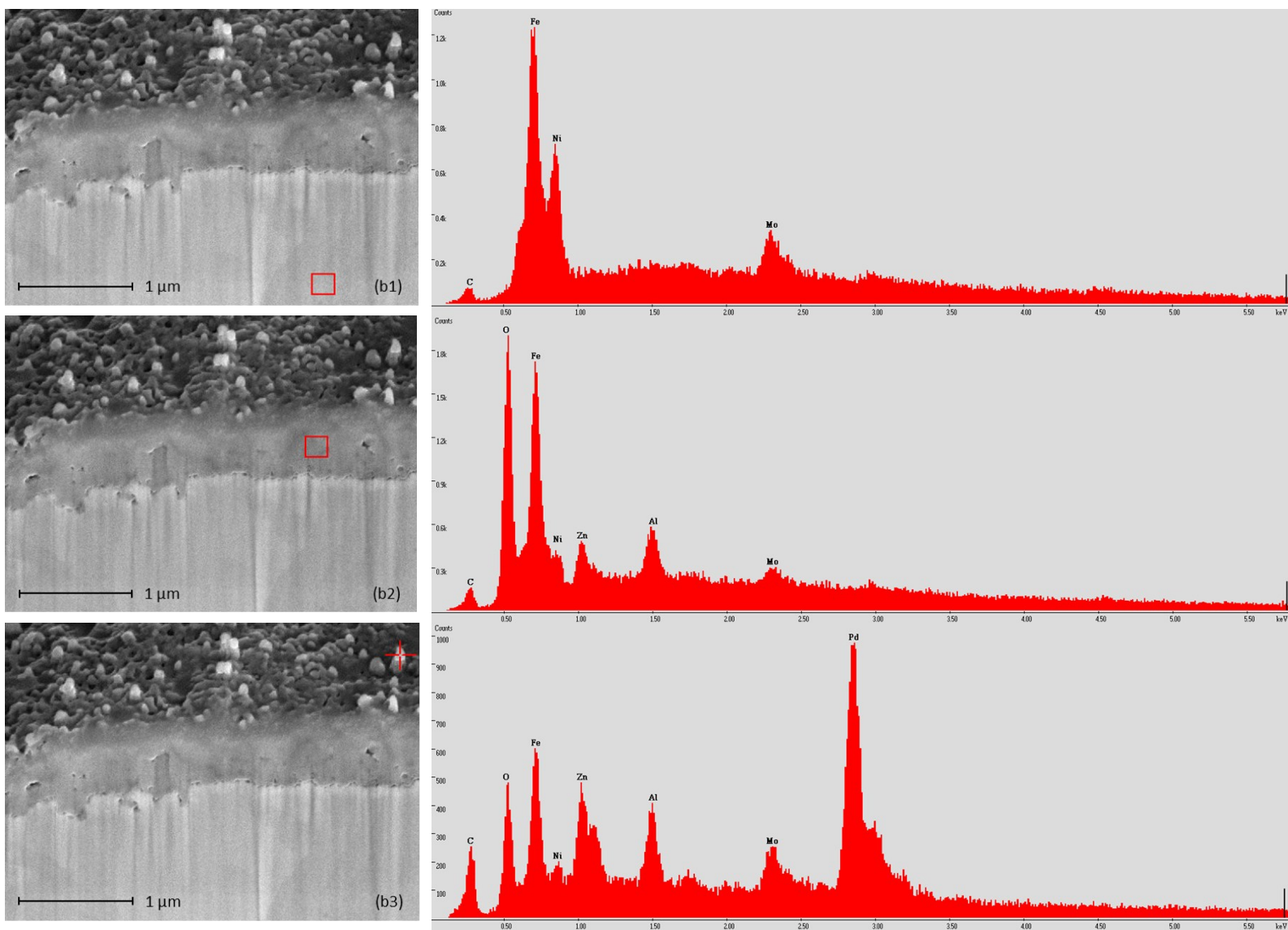


Fig. S1 SEM microphotographs of the cross section of a catalyst particle and their respective EDX spectra.

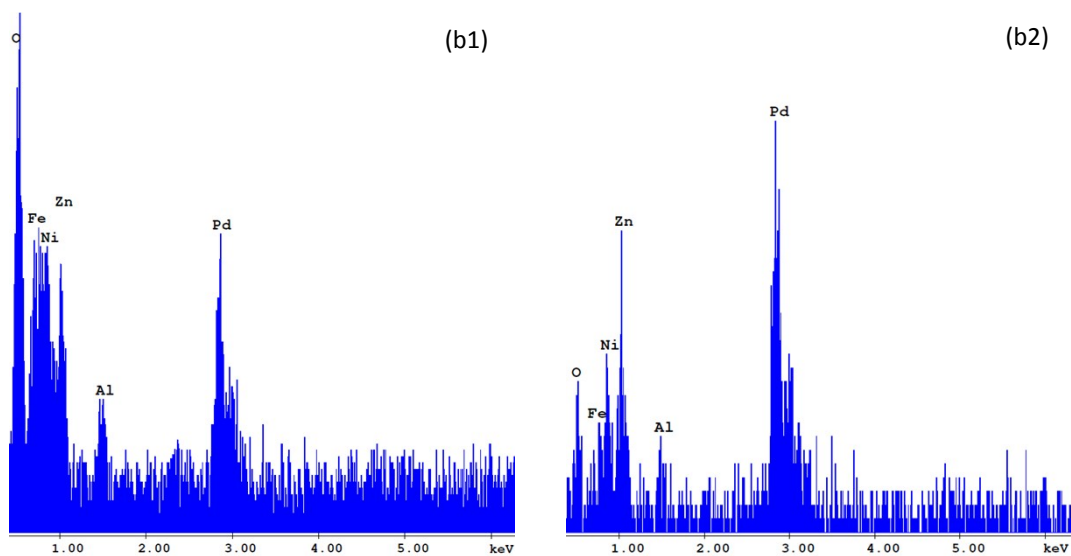
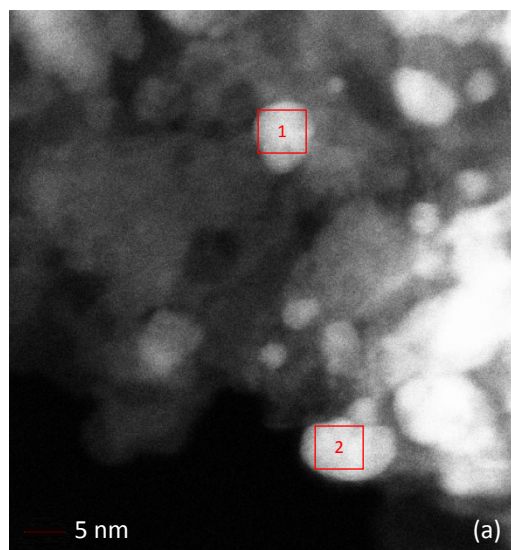


Fig. S2 (a) HAADF-STEM image of the catalyst surface with Pd nanoparticles dispersed on $\text{Al}_2\text{O}_3/\text{ZnO}$. (b1,b2) Sections of EDX spectra recorded respectively at the inspection fields 1 and 2 marked in the image (a).

Fig. S3 (a) shows the TPR profiles obtained before (black) and after (red) the temperature oxidation study depicted in Fig. S3 (b). Higher intensity were observed after the oxidation of the sample. The principal peaks at around 730 K were attributed to the reduction of ZnO. It is reported that ZnO species started to be reduced at 875 K. However, this peak is shifted to lower temperatures when Pd is supported on the surface of ZnO/Al₂O₃.¹ The weak peak at around 330 K (red profile) after the oxidation of the sample can be ascribed to the reduction of PdO to metallic Pd.

The TPO profile shows three peaks at around 640, 760 and 850 K to which it is difficult to ascribe definite oxidation stages. The first peak at around 650 K could be ascribed to Pd oxidation. However, the recorded low signals, ascribed to the low Pd loading of the catalyst, do not make the analysis suitable for quantitative investigations.

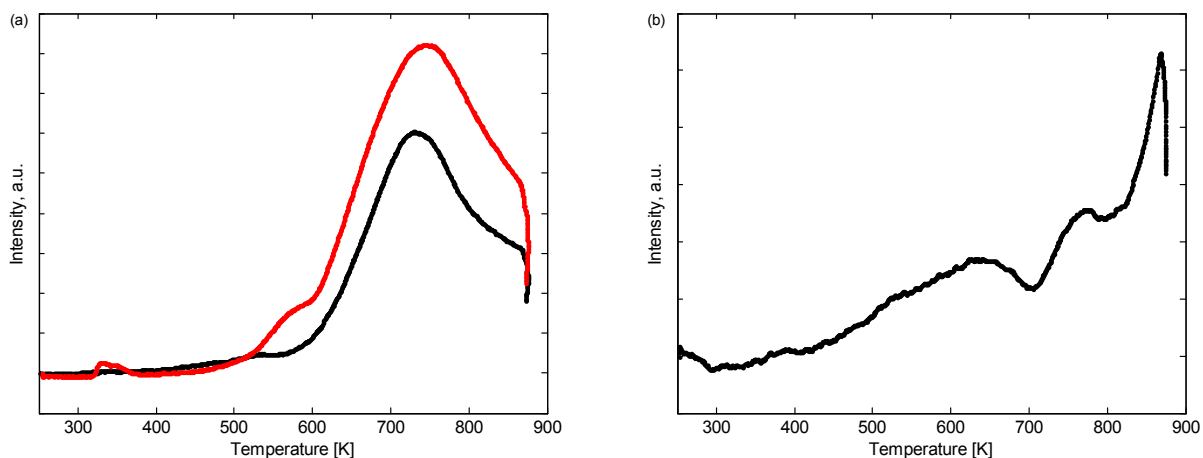


Fig. S3 (a) TPR profiles of Pd/ZnO catalyst before (black) and after (red) temperature oxidation study. (b) TPO profile of Pd/ZnO catalyst.

Mass transfer resistances

Parameters α_1 and α_2 , expressed from eqn (1) and (2), are listed in Table S2. The results allow G-L and L-S mass transfer resistances to be neglected in this study.

Table S2 Summary of experimental and estimated values for the characterization of G-L and L-S mass transfer resistances

Run	T K	p bar	Catalyst loading wt %	$k_L a$ s^{-1}	$k_S a_S$ s^{-1}	$r_0 \cdot 10^3$ $mol \cdot L^{-1} \cdot s^{-1}$	α_1	α_2
1	333	7.0	0.50	0.43	0.28	0.25	0.003	0.004
2	353	7.0	0.50	0.51	0.45	0.48	0.005	0.005
3	333	7.0	0.75	0.43	0.42	0.42	0.005	0.005
4	353	3.0	0.75	0.51	0.68	0.25	0.006	0.004
5	333	10.0	0.50	0.43	0.28	0.33	0.003	0.004
6	333	4.0	0.50	0.43	0.28	0.13	0.002	0.004
7	313	7.0	0.75	0.36	0.24	0.25	0.003	0.005
8	353	7.0	0.25	0.51	0.23	0.27	0.003	0.006
9	313	7.0	0.50	0.36	0.16	0.20	0.003	0.006
10	353	4.0	0.50	0.51	0.45	0.26	0.004	0.005
11	353	9.0	0.50	0.51	0.45	0.65	0.005	0.005
12	333	7.0	0.25	0.43	0.14	0.11	0.001	0.004
13	343	7.0	0.50	0.47	0.36	0.38	0.004	0.005
14	333	5.0	0.75	0.43	0.42	0.27	0.004	0.004

References

- (1) J. Xu, X. Su, X. Liu, X. Pan, G. Pei, Y. Huang, X. Wang, T. Zhang, H. Geng, *Appl. Catal. A*, 2016, 514, 51 – 59.